

Supporting Information

to

**Understanding the stability of amorphous form of darifenacin**

Przemysław Nowak<sup>1,2</sup>, Anna Pietrzak<sup>3</sup>, Marta K. Dudek<sup>1\*</sup>

<sup>1</sup>Centre of Molecular and Macromolecular Studies PAS, Sienkiewicza 112, 90-363 Łódź

<sup>2</sup>BioMedChem Doctoral School of University of Lodz and Institutes of PAS in Lodz, Matejki 21/23, 90-237 Łódź

<sup>3</sup>Institute of General and Ecological Chemistry, Łódź University of Technology, Żeromskiego 114, 90-543 Łódź

<b>Content</b>	<b>page</b>
<b>Table S1.</b> Selected crystallographic data for DAR-H and DAR-T	<b>2</b>
<b>Table S2.</b> Geometrical parameters of hydrogen bonds for DAR-H and DAR-T	<b>2</b>
<b>Table S3.</b> Assignment of the experimental <sup>13</sup> C chemical shifts (δ, ppm) and calculated shielding constant values (σ, ppm) for DAR-H and DAR-T	<b>7</b>
<b>Table S4.</b> Assignment of the experimental <sup>15</sup> N chemical shifts (δ, ppm) and calculated shielding constant values (σ, ppm) for DAR-H and DAR-T	<b>8</b>
<b>Table S5.</b> Gas phase SCF (E <sup>rel</sup> ) and Gibbs free energies (ΔG <sup>rel</sup> ), both in kJ/mol, of the molecular conformations of DAR selected for CSP calculations	<b>12</b>
<b>Figure S1.</b> Packing of molecules and the list of intermolecular interaction in DAR-H	<b>3</b>
<b>Figure S2.</b> <sup>1</sup> H NMR of neat darifenacin in MeOD	<b>4</b>
<b>Figure S3.</b> DSC and TGA plots for DAR-H, DAR-T and DAR-A	<b>5</b>
<b>Figure S4.</b> <i>inv</i> - <sup>1</sup> H- <sup>13</sup> C HETCOR with long second contact time and <sup>1</sup> H- <sup>1</sup> H SQ-DQ Back-to-back correlation NMR spectra for DAR-H	<b>6</b>
<b>Figure S5.</b> FT-IR spectra for DAR-H, DAR-T and DAR-A, with the expanded regions showing C=O stretching, NH <sub>2</sub> bending, and NH <sub>2</sub> stretching bands.	<b>8</b>
<b>Figure S6.</b> PXRD for DAR crystallized from isopropanol (DAR-H), DAR-H after 10 months of storage and DAR-H after thermal treatment.	<b>10</b>
<b>Figure S7.</b> PXRD for DAR-T crystallized from undried toluene, DAR-T after 6 months of storage and DAR-T after thermal treatment	<b>10</b>
<b>Figure S8.</b> PXRD for DAR-A after desalination, after 5 months of storage at ambient conditions, and after keeping DAR-A in a jar with toluene vapour for 10 days	<b>11</b>
<b>Figure S9.</b> PXRD for DAR-A after keeping it in a humidity chamber for 2-22h.	<b>11</b>
<b>Figure S10.</b> Bent conformations of DAR representing gas phase minima taken for CSP calculations.	<b>13</b>
<b>Figure S11.</b> Extended conformations of DAR representing gas phase minima taken for CSP calculations.	<b>14</b>
<b>Figure S12.</b> The frequency of occurrence of individual interactions that stabilize the CSP-predicted low energy structures of neat DAR and DAR monohydrate.	<b>15</b>

## 1. Additional crystallographic data for DAR-H and DAR-T

**Table S1.** Selected crystallographic data for DAR-H and DAR-T

	<b>DAR-H</b> <b>CCDC: 2406917</b>	<b>DAR-T</b> <b>CCDC: 2406918</b>
Empirical formula	C <sub>28</sub> H <sub>30</sub> N <sub>2</sub> O <sub>2</sub> ·0.637(H <sub>2</sub> O)	C <sub>28</sub> H <sub>30</sub> N <sub>2</sub> O <sub>2</sub> ·C <sub>7</sub> H <sub>8</sub>
Formula weight	437.99	518.67
Temperature/K	100(2)	99.99(10)
Crystal system	triclinic	Monoclinic
Space group	<i>P</i> 1	<i>P</i> 2 <sub>1</sub>
Cell lengths [Å]	a=6.804(3) b=8.815(3) c=10.484(4)	a=12.236(4) b=8.787(3) c=14.035(4)
Cell angles [°]	α=88.30(3) β=88.30(3) γ=69.87(3)	α=90 β=113.02(3) γ=90
Cell volume [Å <sup>3</sup> ]	590.12(4)	1388.98
Z	1	2
Z'	1	1
Crystal size/mm <sup>3</sup>	0.22 x 0.18 x 0.12	0.22 x 0.1 x 0.04
Radiation	CuKα (λ = 1.54184)	CuKα (λ = 1.54184)
2θ range for data collection/°	8.44 to 153.228	6.842 to 153.838
Index ranges	-8 ≤ h ≤ 8, -10 ≤ k ≤ 11, -13 ≤ l ≤ 12	-15 ≤ h ≤ 14, -10 ≤ k ≤ 11, -17 ≤ l ≤ 16
Reflections collected	21405	37677
Independent reflections	4406 [R <sub>int</sub> = 0.0467, R <sub>sigma</sub> = 0.0321]	5409 [R <sub>int</sub> = 0.0643, R <sub>sigma</sub> = 0.0336]
Data/restraints/parameters	4406/3/311	5409/213/400
Goodness-of-fit on F <sup>2</sup>	1.065	1.066
Final R indexes [I > 2σ (I)]	R <sub>1</sub> = 0.0357, wR <sub>2</sub> = 0.0910	R <sub>1</sub> = 0.0446, wR <sub>2</sub> = 0.0950
Final R indexes [all data]	R <sub>1</sub> = 0.0372, wR <sub>2</sub> = 0.0922	R <sub>1</sub> = 0.0501, wR <sub>2</sub> = 0.0971
Largest diff. peak/hole/e Å <sup>-3</sup>	0.18/-0.18	0.20/-0.18

**Table S2.** Geometrical parameters of hydrogen bonds for DAR-H and DAR-T.

Hydrogen bond	D-H [Å]	H···A [Å]	D···A [Å]	D-H···A [Å]
<b>DAR-H</b>				
N <sub>2</sub> -H <sub>2A</sub> ···O <sub>3</sub>	0.929	2.691	3.561	134.72
O <sub>3</sub> -H <sub>3A</sub> ···O <sub>2</sub>	0.872	2.188	3.052	170.70

$N_2-H_{2B} \cdots N_1$	0.942	1.977	2.897	164.74
<b>DAR-T</b>				
$N_2-H_{2A} \cdots N_1$	0.877	2.155	2.997	160.61
$N_2-H_{2B} \cdots O_1$	0.904	2.602	3.410	149.09

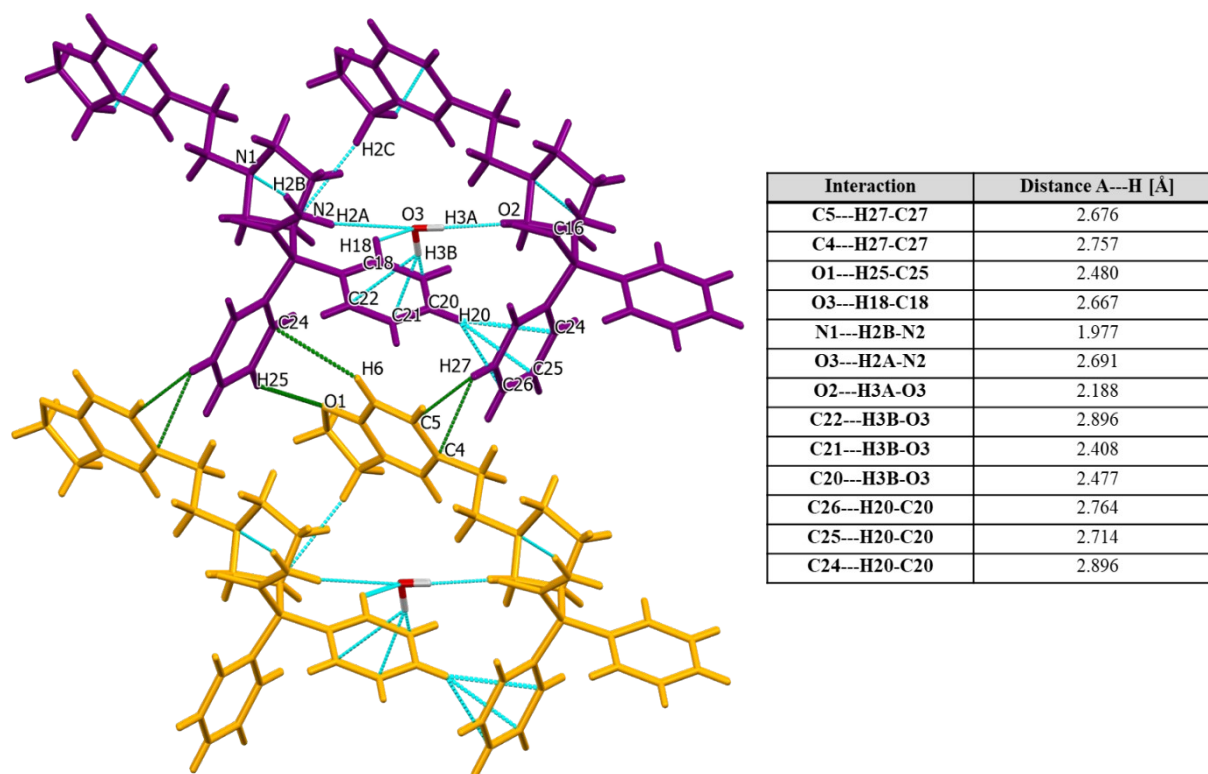


**Figure S1.** Packing of molecules and the list of intermolecular interaction in DAR-H. DAR layers are marked with different colours. Hydrogen bonds and other interactions in the layer are highlighted in blue. Interactions that stitch the layers together are highlighted in green.

Structure DAR-H co-crystallized non stoichiometric number of water molecules in asymmetric unit. The occupancy is refined to 0.64(1). The void space (30 Å<sup>3</sup>) and electron count (7 e<sup>-</sup>) calculated using SQUEEZE tool [1] exposed the content of water. The SQUEEZE tool has been used only to verify information about water content. The DAR-H deposited CIF file contains the refined water molecule model, not SQUEEZED. Structure DAR-T contains molecules of toluene disordered over two positions with occupancy ratio refined to 0.745(6):0.255(8). The disorder was refined using set of restraints and constraints for a toluene fragment as implemented in DSR [2] plugin in ShelXle [3]. Additionally, AFIX 66 and DFIX for the ring to methyl carbon and SIMU for the ADPs has been used.

## 2. Spectral data for amorphous DAR (<sup>1</sup>H NMR and MS)

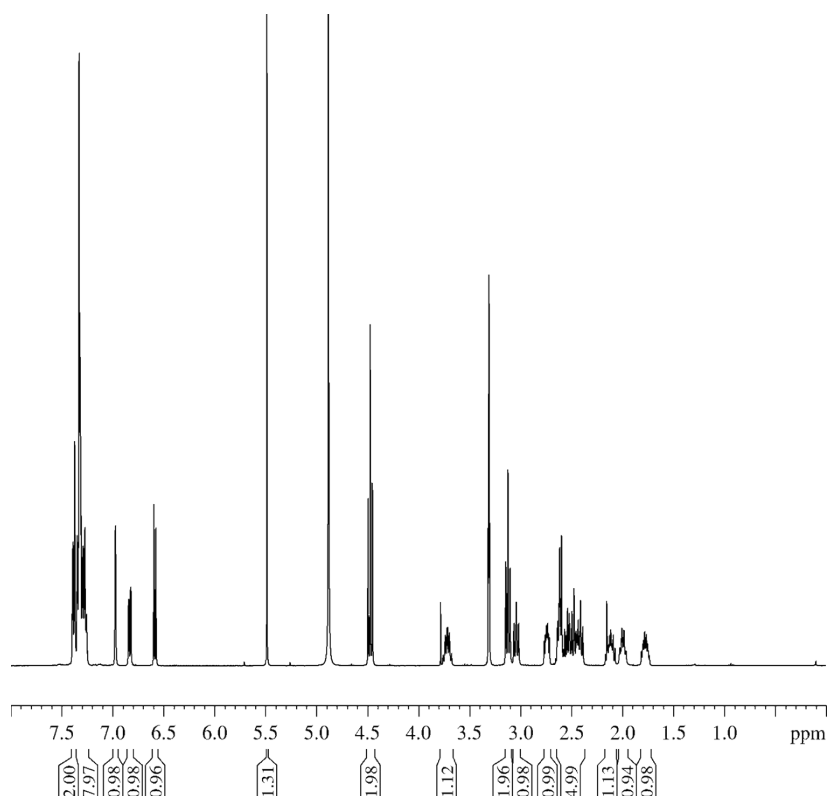


**Figure S2.** <sup>1</sup>H NMR of neat darifenacin in MeOD.

High-resolution mass spectrometry (HRMS) was used to confirm the darifenacin molecular formula. Calculated  $m/z$  for  $[M+H]^+$  pseudomolecular darifenacin ion ( $C_{28}H_{31}N_2O_2$ ) was 427.2386 and found mass was 427.2390. HRMS measurements were performed using a Synapt G2-Si mass spectrometer (Waters) equipped with an ESI source and quadrupole-time-of-flight mass analyzer. The mass spectrometer was operated in the positive ion detection mode.

### 3. Additional spectral, thermal and diffraction data for solid forms of DAR

#### a. DSC and TGA plots

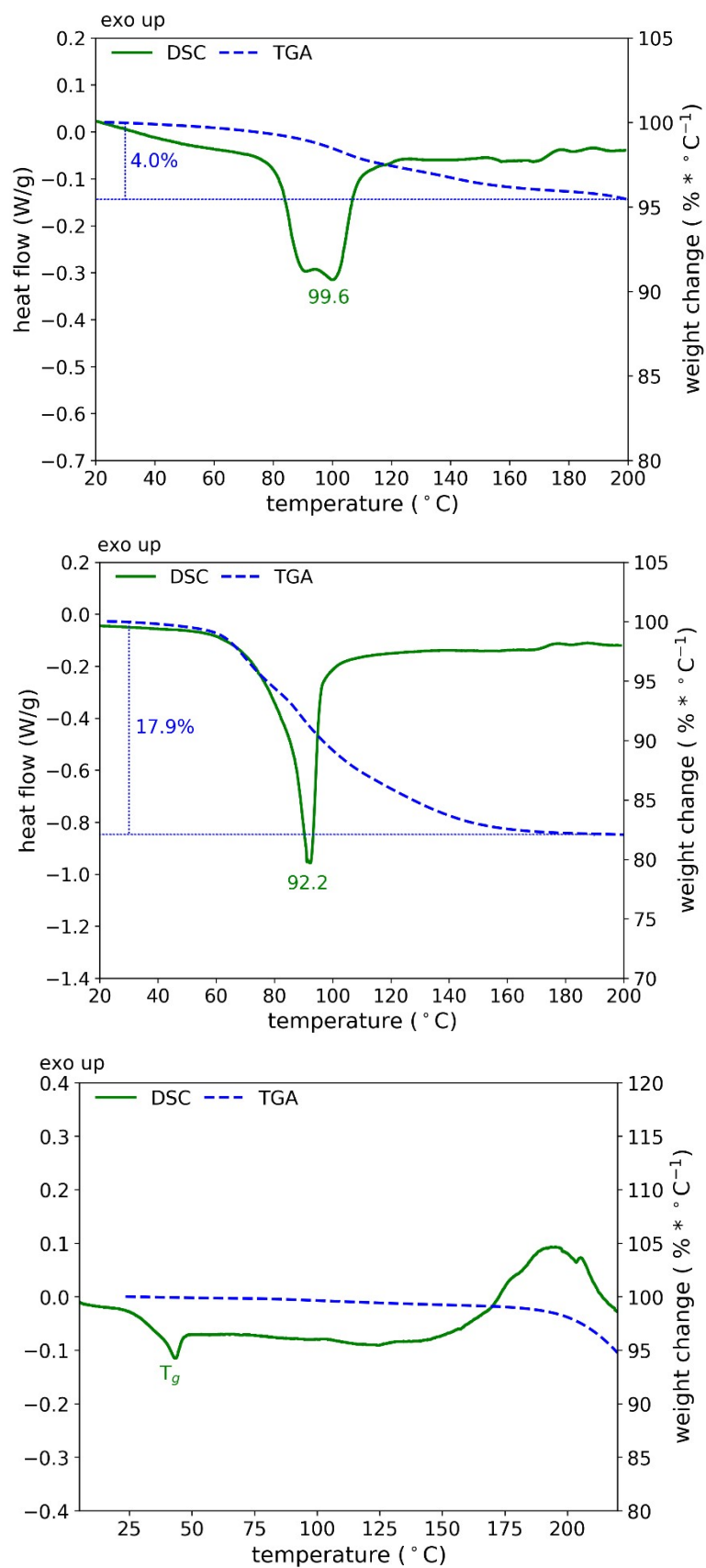
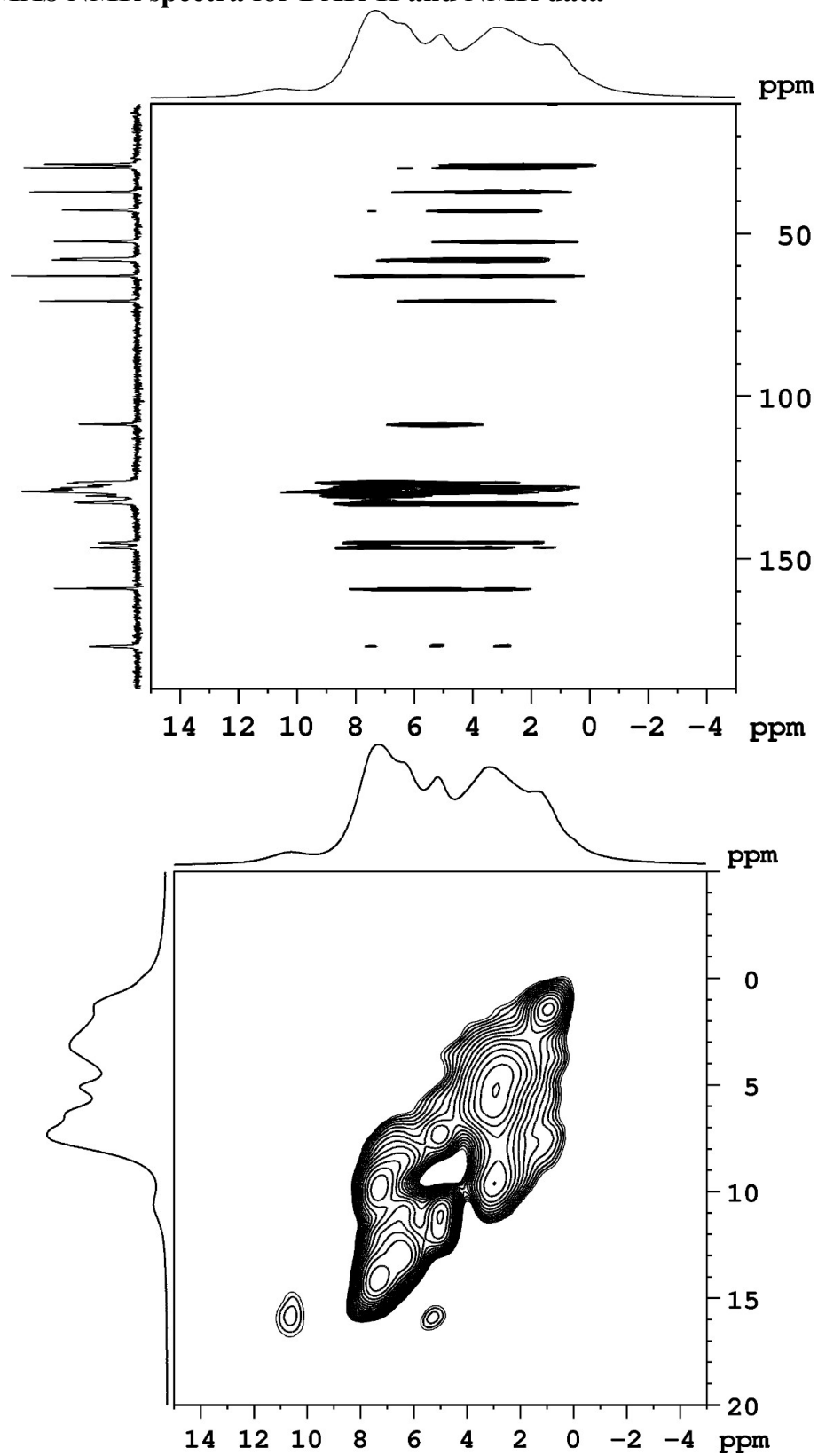


Figure S3. DSC and TGA plots for DAR-H, DAR-T and DAR-A

**b. VF MAS NMR spectra for DAR-H and NMR data**



**Figure S4.**  ${}^{\text{inv-}}{}^1\text{H}$ - ${}^{13}\text{C}$  HETCOR with long second contact time (upper) and  ${}^1\text{H}$ - ${}^1\text{H}$  SQ-DQ Back-to-back (lower) correlation NMR spectra for DAR-H

**Table S3.** Assignment of the experimental  $^{13}\text{C}$  chemical shifts ( $\delta$ , ppm) and calculated shielding constant values ( $\sigma$ , ppm) for DAR-H and DAR-T. For shielding constants of DAR-T the average values weighted over the two site occupancies of toluene molecule are given.

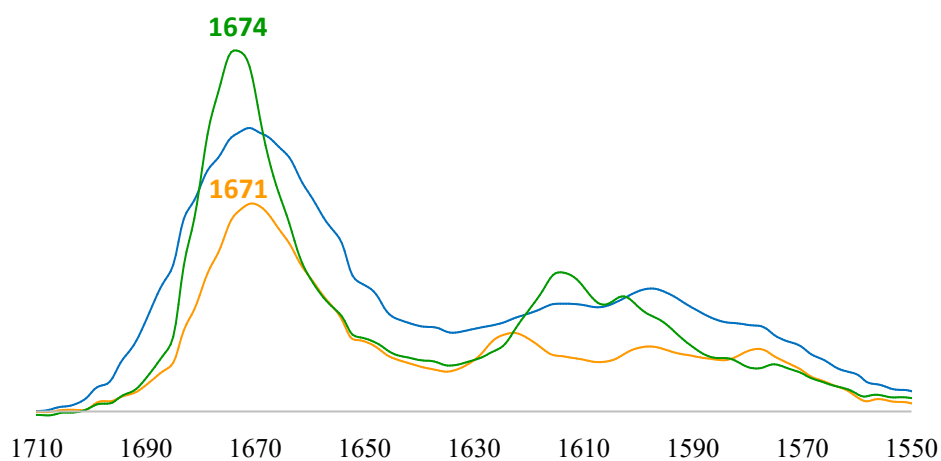
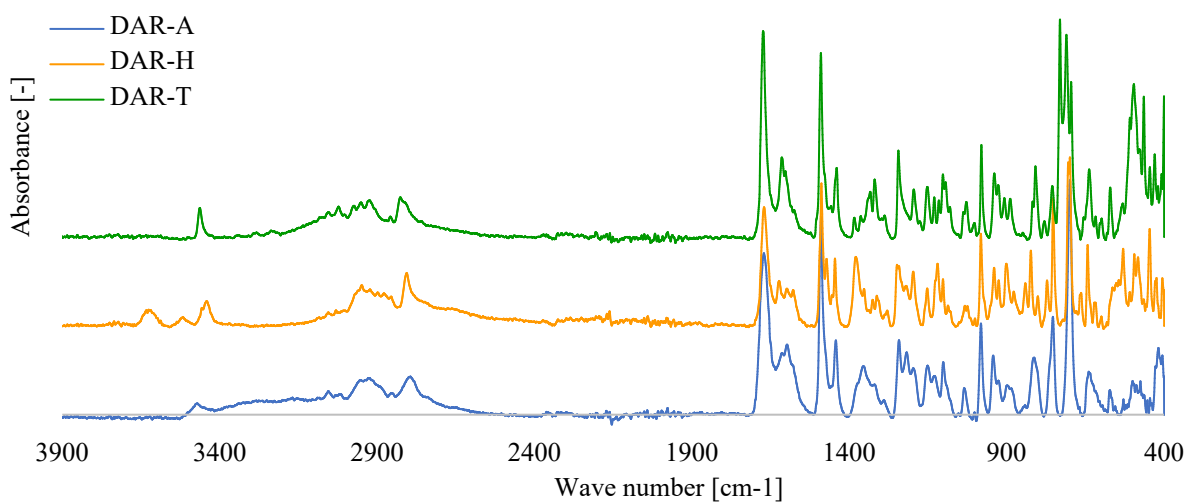
atom no.	DAR-H		DAR-T	
	$\delta(^{13}\text{C})$	$\sigma(^{13}\text{C})$	$\delta(^{13}\text{C})$	$\sigma(^{13}\text{C})$
C1	70.6	98.46	70.4	98.31
C2	29.5	143.42	29.7	142.43
C3	128.2	41.39	125.9	44.05
C4	132.6	38.45	133.4	36.64
C5	128.5	40.75	129.4	40.15
C6	108.5	63.92	109.9	61.75
C7	159.1	9.3	158.0	10.46
C8	127.5	40.49	127.5	42.22
C9	37.0	135.2	34.6	139.91
C10	57.5	115.74	60.6	111.52
C11	57.9	114.93	58.4	114.70
C12	42.6	128.53	40.8	131.35
C13	28.6	146.01	26.4	148.12
C14	52.2	120.3	52.4	121.76
C15	62.8	106.69	64.8	103.00
C16	176.9	-6.66	176.2	-5.78
C17	145.1	23.43	143.5	25.31
C18	129.2	40.46	130.5	39.02
C19	129.2	38.2	127.9	41.71
C20	126.7	42.7	127.9	41.80
C21	126.4	43.01	129.0	41.47
C22	130.6	36.56	131.0	38.50
C23	146.5	21.41	143.5	23.92
C24	126.7	41.42	135.7	33.21
C25	128.2	41.15	127.5	41.81
C26	126.4	43.4	126.7	42.34
C27	129.2	38.13	126.7	43.78
C28	128.5	40.63	132.2	37.55
C1T			137.6	29.55
C2T			129.0	40.89
C3T			129.4	39.54
C4T			125.9	44.31
C5T			127.9	41.79

C6T	126.7	42.45
C7T	21.8	152.04

**Table S4.** Assignment of the experimental  $^{15}\text{N}$  chemical shifts ( $\delta$ , ppm) and calculated shielding constant values ( $\sigma$ , ppm) for DAR-H and DAR-T. For shielding constants of DAR-T the average values weighted over the two site occupancies of toluene molecule are given.

atom no.	DAR-H		DAR-T	
	$\delta(^{15}\text{N})$	$\sigma(^{15}\text{N})$	$\delta(^{15}\text{N})$	$\sigma(^{15}\text{N})$
$\text{N}_{\text{ring}}$	59.5	163.27	54.2	168.47
$\text{NH}_2$	119.0	96.82	106.2	111.40

### c. FT-IR spectra



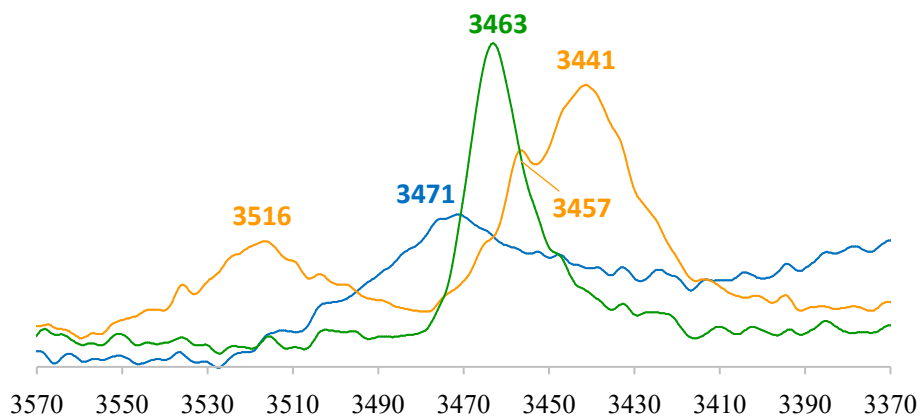


**Figure S5.** FT-IR spectra for DAR-H, DAR-T and DAR-A, with the expanded regions showing C=O stretching (ca. 1670  $\text{cm}^{-1}$ ) and  $\text{NH}_2$  bending (1640-1570  $\text{cm}^{-1}$ ), and  $\text{NH}_2$  stretching bands (3540-3420  $\text{cm}^{-1}$ ).

#### d. PXRD plots

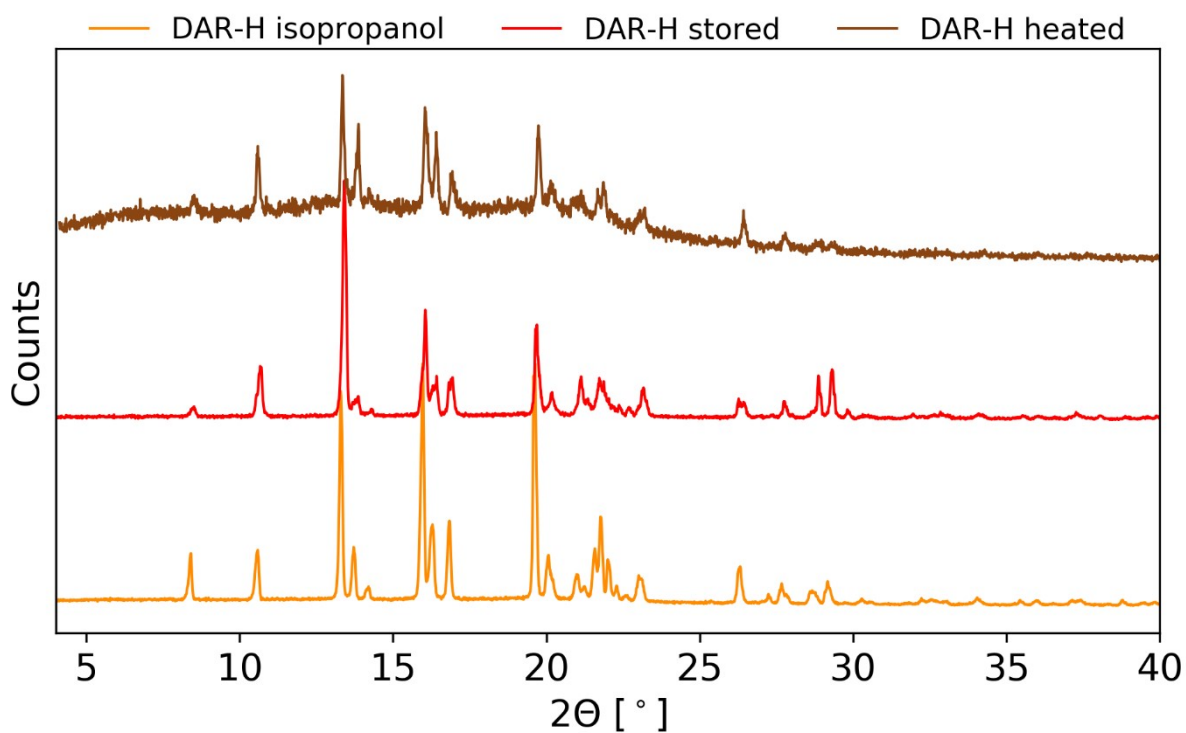


**Figure S6.** PXRD for DAR crystallized from isopropanol (DAR-H), DAR-H after 10 months of storage and DAR-H after thermal treatment (4h at 90 °C).

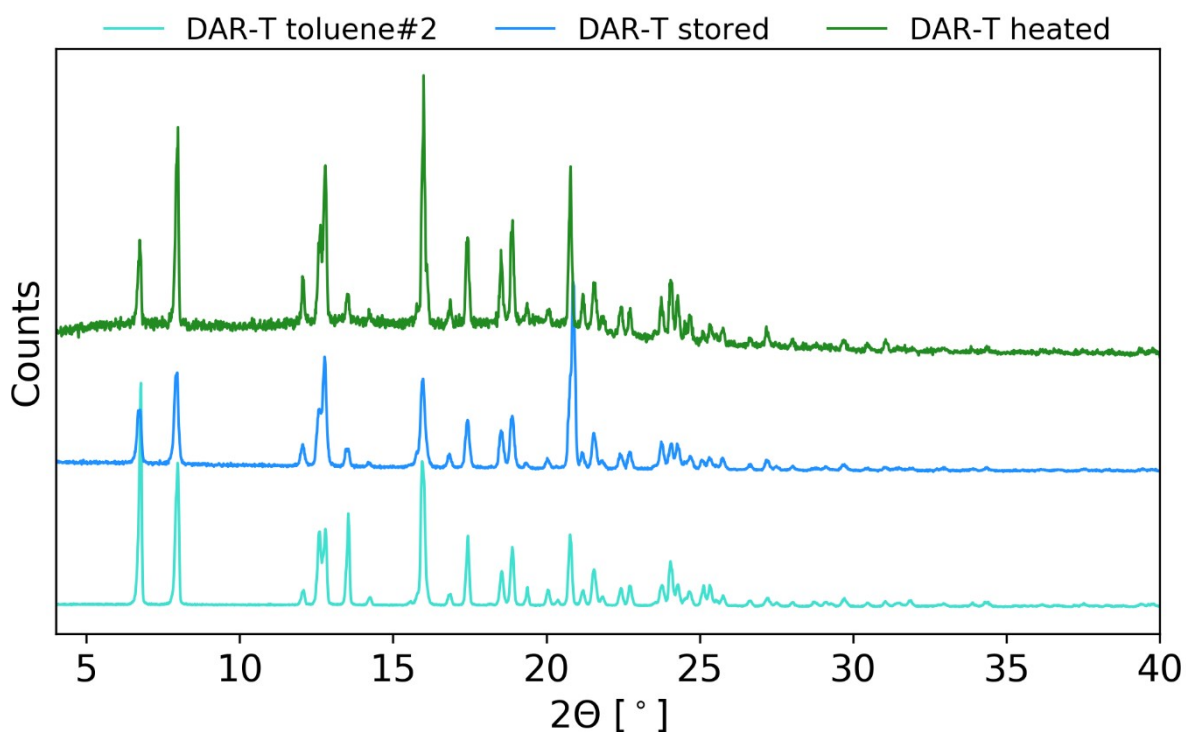


**Figure S7.** PXRD for DAR-T crystallized from undried toluene (crystallization after DAR-T was once obtained through crystallization in a freezer), DAR-T after 6 months of storage and DAR-T after thermal treatment (30 min at 80 °C).

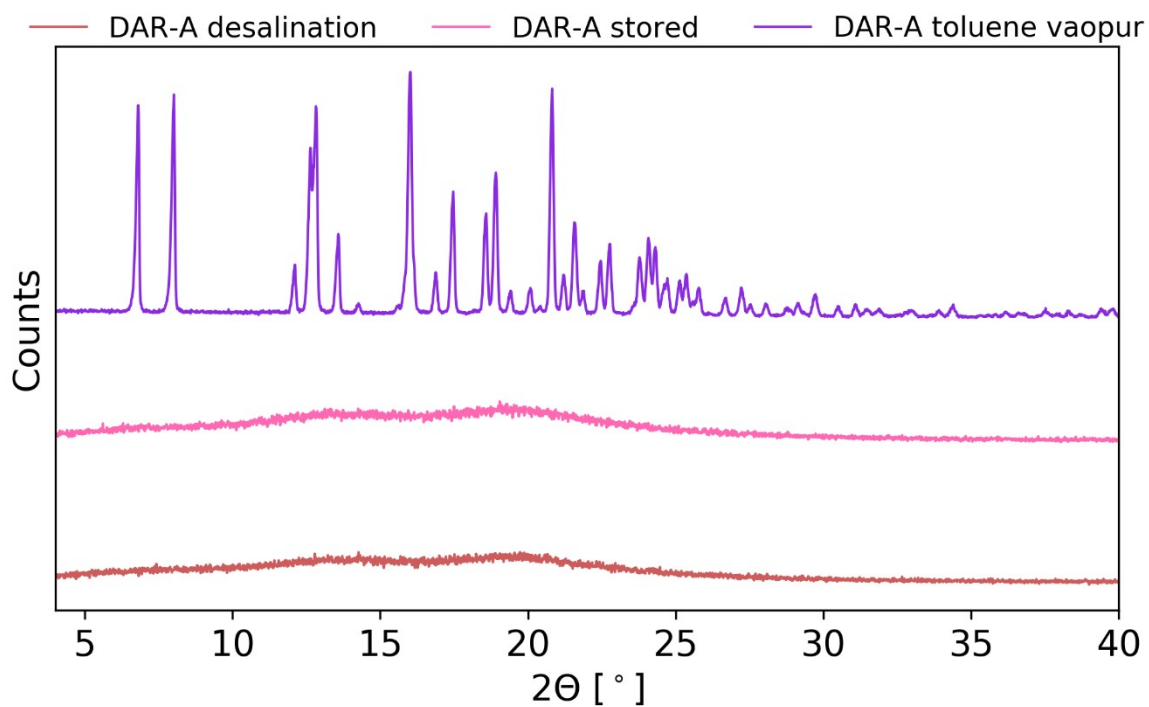


**Figure S8.** PXRD for DAR-A after desalination, after 5 months of storage at ambient conditions, and after keeping DAR-A in a jar with toluene vapour for 10 days.

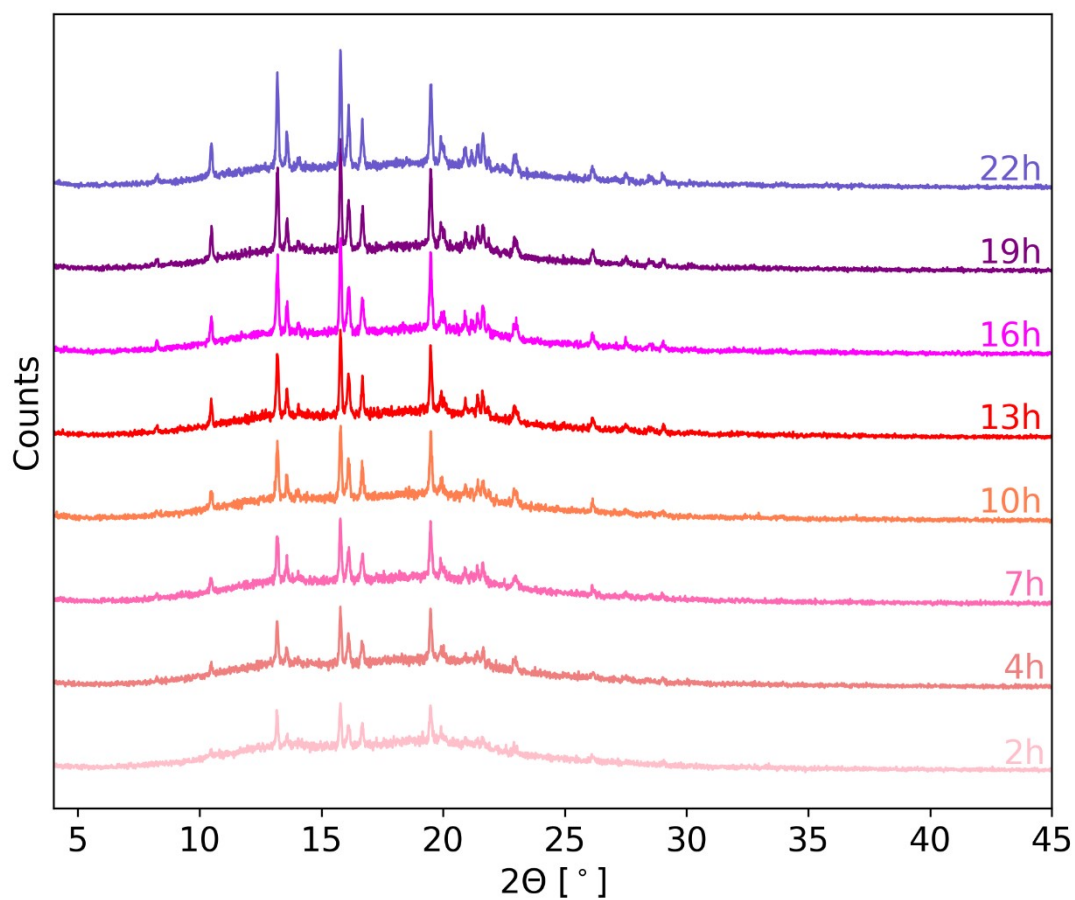


**Figure S9.** PXRD for DAR-A after keeping it in a humidity chamber ( $T = 35\text{ }^\circ\text{C}$ ,  $\text{RH} = 95\%$ ). The diffractograms were registered at ca. 3-hour intervals.

## 4. Theoretical results

### a. Conformational search results

**Table S5.** Gas phase SCF ( $E^{\text{rel}}$ ) and Gibbs free energies ( $\Delta G^{\text{rel}}$ ), both in kJ/mol, of the molecular conformations of DAR selected for CSP calculations.

conformation	$E^{\text{rel}}$	$\Delta G^{\text{rel}}$	intramolecular interaction (if any)
df100	0.00	0.00	NH2...O
df63	6.84	0.92	Ar-H...O
df134	8.56	9.10	NH2...O
df122	8.57	8.39	NH2...O
df38	9.11	3.05	Ar-H...O
df36	9.14	3.42	Ar-H...O
df113	9.90	6.08	Ar-H...O
df142	11.17	6.68	Ar-H...O
df112	11.49	8.85	NH2...O
df41	12.59	4.99	Ar-H...O
df117	13.20	9.69	NH2...O
df35	14.04	7.84	Ar-H...O
df33	15.42	9.65	Ar-H...O
df29	16.21	8.88	CH2...pi
df54	22.22	6.31	
df67	22.97	7.13	
df59	23.17	6.85	
df79	24.04	8.20	
df4	24.51	9.16	
df6	24.82	9.69	
df43	25.32	9.91	
df71	25.85	8.08	
df13	25.87	9.96	

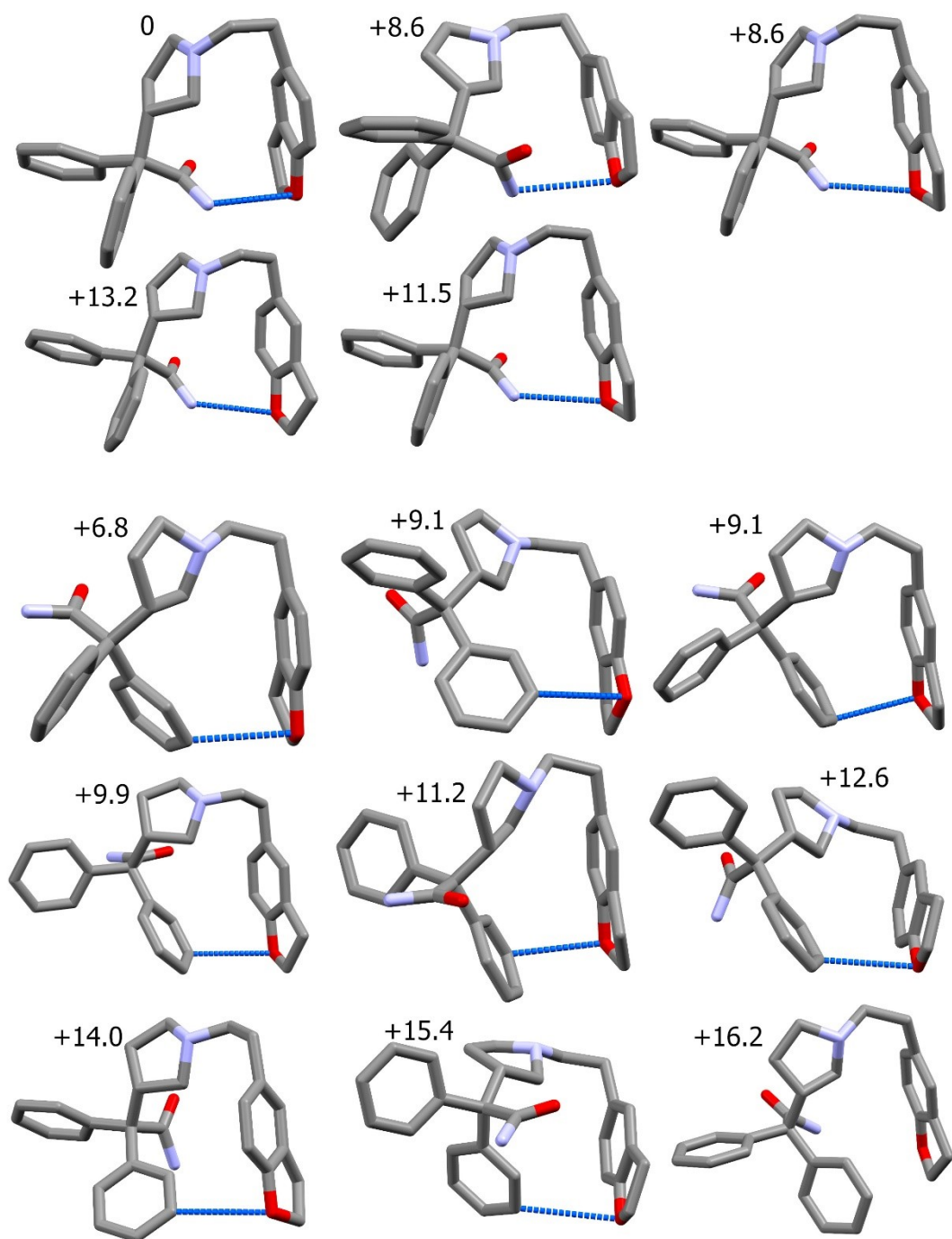


**Figure S10.** Bent conformations of DAR representing gas phase minima taken for CSP calculations. The numbers denote relative energy in respect to the global gas phase minimum conformation shown in top left corner.

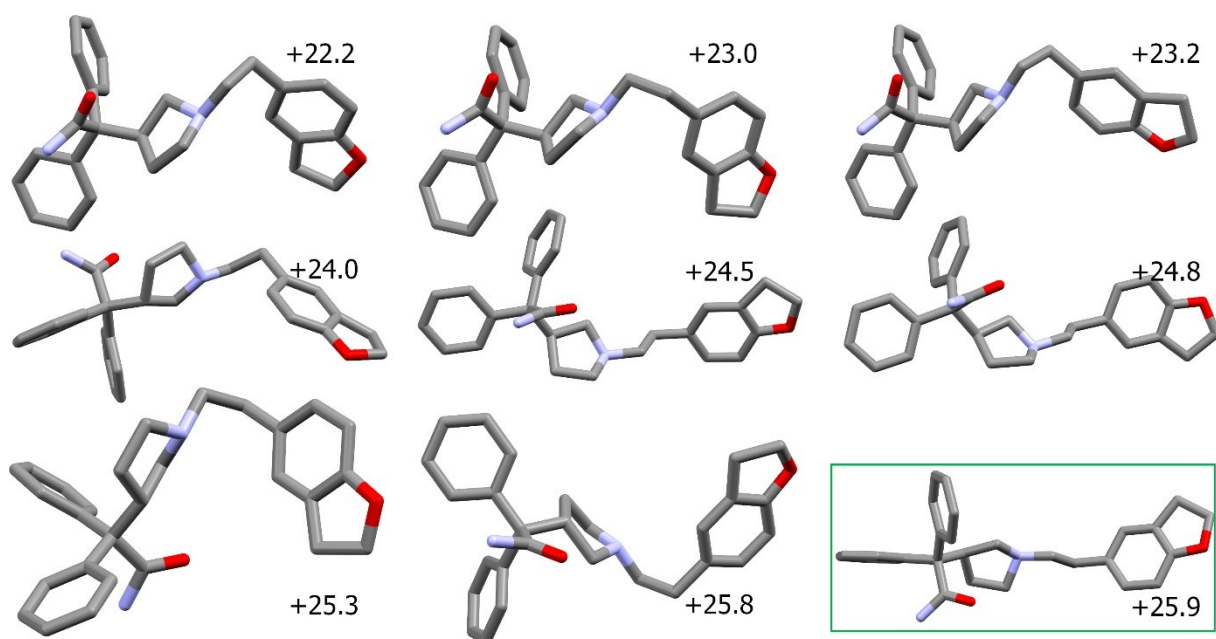


**Figure S11.** Extended conformations of DAR representing gas phase minima taken for CSP calculations. The numbers denote relative energy in respect to the global gas phase minimum conformation shown in top left corner in Figure S9. Green rectangle marks gas phase minimum conformation similar to that building the experimental crystal structure of DAR hydrate.

### **b. comparison of the stabilizing interactions in neat and hydrated structures**

Figure S11 shows a comparison of the most important stabilizing interactions of the low energy structures from CSP calculations for neat DAR and DAR monohydrate. The most important interactions in both structures are CH- $\pi$  interactions are formed between aromatic rings or aromatic rings and alkyl CH groups. However, for structures of neat DAR the next most abundant stabilizing interactions are weaker NH- $\pi$  interactions, as well as hydrogen bonds between neighbouring molecules of DAR ( $\text{NH}_2 \dots \text{N}$ ), which requires an extended, not energetically favourable conformation to be present. In contrast, in DAR monohydrate structures there is an abundance of intermolecular interactions with water molecule, which play a crucial role in energetic compensation of a loss caused by the presence of an extended conformation.

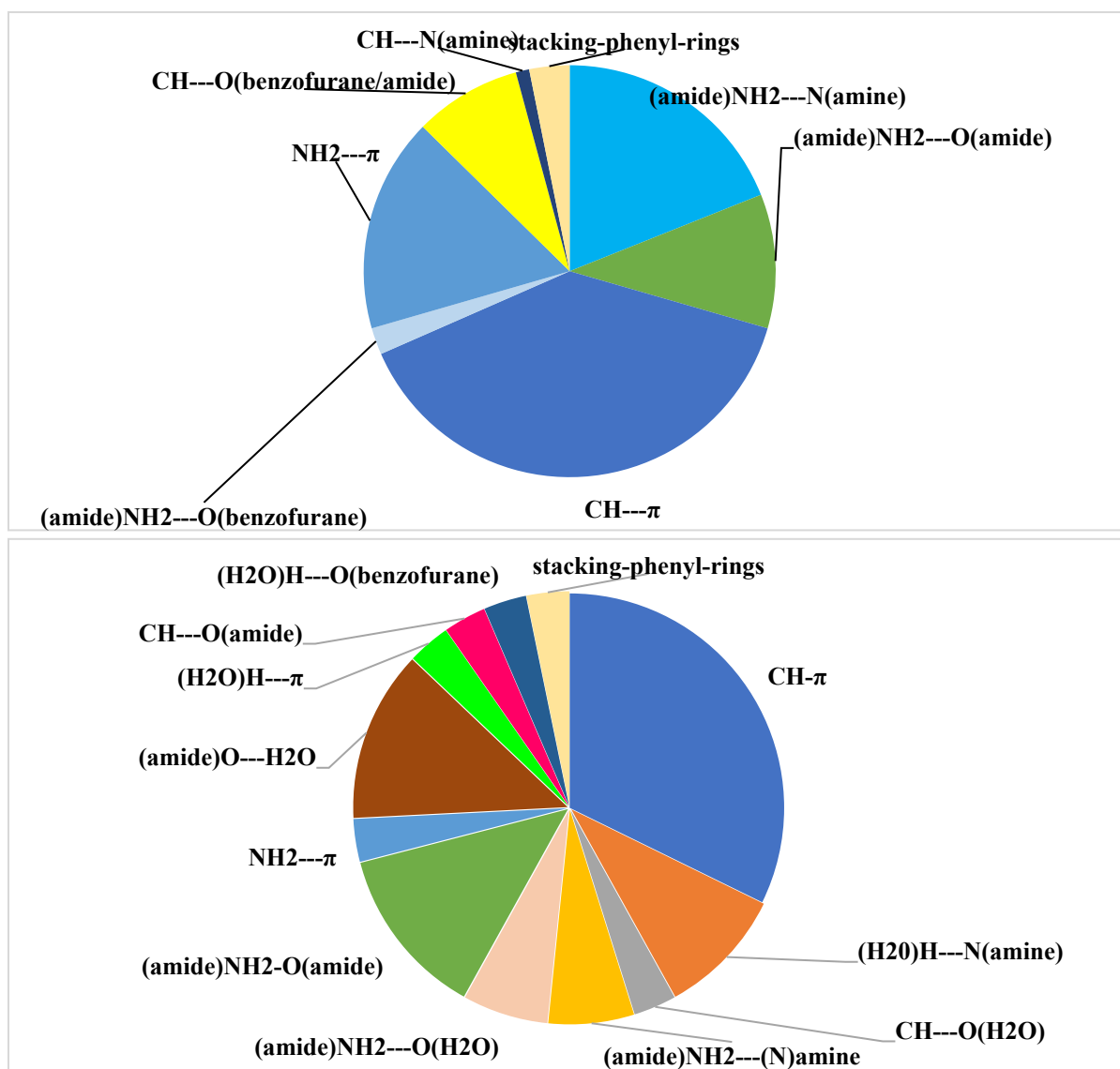


**Figure S12.** The frequency of occurrence of individual interactions that stabilize the CSP-predicted low energy structures of neat DAR(upper) and DAR monohydrate (lower).

## References

- [1] A. L. Spek. PLATON SQUEEZE: a tool for the calculation of the disordered solvent contribution to the calculated structure factors. *Acta Cryst.* **2015**, C71, 9-18.
- [2] D. Kratzert and I. Krossing. Recent improvements in DSR. *J. Appl. Cryst.* **2018**, 51, 928-934.
- [3] C. B. Hübschle, G. M. Sheldrick and B. Dittrich. ShelXle: a Qt graphical user interface for SHELXL. *J. Appl. Cryst.* **2011**, 44, 1281-1284.